Desalination and Water Treatment
www.deswater.com
doi: 10.1080/19443994.2015.1030701

57 (2016) 9383–9395
April

Taylor & Francis
Taylor & Francis Group

Lead(II) removal from aqueous solutions by organic thiourea derivatives intercalated magadiite

Soumia Benkhatou[a,b], Amal Djelad[b], Mohamed Sassi[b,*], Mohamed Bouchekara[c], Abdelkader Bengueddach[b]

[a]*Laboratoire de Matériaux Application à l'Environnement, Sciences and Technologies, University of Mascara, BP305 route de Mamounia, 29000 Mascara, Algeria, Tel. +213 792134147; email: soumia.benkhatou@gmail.com*
[b]*Laboratoire de Chimie des Matériaux – Département de Chimie, University of Oran1 Ahmed Benbella, BP 1524 El-Menaouer, 31000 Oran, Algeria, Tel. +213 794707060, email: djelad_am@yahoo.fr (A. Djelad), Tel. +213 665003348; Fax: +213 41299998; email: sassim2006@yahoo.fr (M. Sassi), Tel. +213 558047969; email: abengueddach@gmail.com (A. Bengueddach)*
[c]*Laboratoire de Chimie Organique Macromoléculaire et Matériaux – Sciences and Technologies, University of Mascara, BP305 route de Mamounia, 29000 Mascara, Algeria, Tel. +213 775154140; email: ybouchekara@yahoo.fr*

Received 5 May 2014; Accepted 7 March 2015

ABSTRACT

In this work, a layered silicate magadiite-Na (Mag) is hydrothermally synthesized and used to prepare organic thiourea-intercalated magadiite. It is organically modified by N-(2-methoxyphenyl)-N′-(2-methylphenyl)-thiourea (TMMe) and N-(2-methoxyphenyl)-N′-(2-methoxyphenyl)-thiourea (TMM) without preintercalation with a cationic surfactant. These materials are characterized by X-ray diffraction, infrared spectroscopy, and scanning electron microscopy. Due to the increment of basic centers attached to the pendant chains, the metal adsorption capacities of the final chelating materials are found to be higher than the precursor. The ability of these materials to remove Pb(II) from an aqueous solution is followed by a series of adsorption isotherms at a temperature of 25°C, pH 5 and pH 7. The kinetic parameters analyzed by the Lagergren and Ho and Mc Kay models give a good fit for a pseudo-second-order reaction for all systems. The adsorption isotherm data follow the Langmuir equation where parameters are calculated. Mag/TMM has a better lead(II) removal capacity (33.44 mg/g) at pH 5 than Mag/TMMe (19.9 mg/g) and Mag (9.91 mg/g) at pH 7.

Keywords: Na-magadiite; Hydrothermal synthesis; Intercalation; Thiourea derivatives; Lead; Adsorption

1. Introduction

Industrial activities produce liquid effluents containing hazardous chemical species for human beings and its direct environment. We can encounter heavy metals among these species, well known for their high toxicity and non-biodegradability. Heavy metals and particularly lead(II) has the most damaging effect on human health [1]. Acute lead(II) poisoning is a major cause for severe kidneys, liver and brain dysfunction, as it may affect the central nervous system [2,3]. Therefore, it is of major importance to control the concentration of heavy metals in industrial waste before

*Corresponding author.

its disposal in the environment [2] and to find a way one can get rid of such waste.

Conventional technologies for the removal of heavy metals from industrial waste involve ion exchange, chemical precipitation, reverse osmosis, solvent extraction, electrodialysis, and membrane separation [3–10]. These methods are expensive as they may have other weaknesses, such as incomplete metal removal, limited tolerance to pH change, moderate or non-metal selectivity, very high or low working levels of metals and production of toxic sludge or other waste products that also need disposal [11]. On the contrary, adsorption is an effective and economical method among the physicochemical treatments [12,13]. Studies on low-cost materials as potential adsorbents have included magadiite, zeolites, chitosan, and agricultural wastes [14].

Magadiite is a part of hydrous layered silicates family, which is also constituted by kenyaite, makatite, and kanemite [15]. Magadiite was first found in the deposits of lake Magadi in Kenya and described by Eugster 1967 [16]. Magadiite is a layered silicate with the ideal formula $Na_2Si_{14}O_{29}{\cdot}nH_2O$ [17] in which the structure of this mineral is composed of one or multiple negatively [15] charged sheets of SiO_4 tetrahedral where the negative charge is compensated by interlayer hydrated sodium ions [18]. The surface of magadiite contains silanol group (Si-OH) and siloxide group ($Si–O^-Na^+$). The interlayer space contains sodium ions and water molecules. Na-magadiite can also be prepared in a laboratory under hydrothermal conditions [19]. It has some specific properties, such as a high capacity for ion exchange compared with smectites [20], interlamellar adsorption of water and polar organic molecules [21], organosilane grafting [18,22], and transformation into crystalline layered silicic acids by proton exchange [15]. These specific properties could promote its application as cation exchanger or molecular sieves [18], adsorbents for environmental pollutants [23,24] and supports for catalyst [25].

The most important characteristics of lamellar solids are the possibility to expand their interlayer space. Indeed, the latter accommodate over a large variety of organic molecules to form intercalated host–guest compounds, for various applications. For example, the intercalation of Na-magadiite with shorter organic cations such as tetrapropylammonium (TPA) is used as intermediate to prepare zeolite materials [26].

The intercalation with longer organic cations such as dodecyltrimethylammonium enhances the silylation of the interlayer space of magadiite [22]. The resulting compounds can be then used as precursors for pillaring reactions and formation of polymer–inorganic nanocomposites [27,28]. Recently, these materials were successfully used to remove heavy metals such as: uranyl(II) [23], arsenic(V) [24], and uranyl(VI) [29,30]. Magadiite is used as an adsorbent for dye removal from aqueous solutions [31]. In this case, the adsorption is carried out by conventional ion exchange processes [32,33].

In the present work, a synthetic Na-magadiite material is organically modified with organic thiourea derivatives. The materials obtained are characterized by X-ray diffraction (XRD), scanning electron microscopy (SEM) and infrared FTIR spectroscopy and used in lead(II) adsorption which is carried out as a function of pH and contact time. The Langmuir and Freundlich adsorption isotherm models are applied in order to fit the experimental data in linear regression.

2. Materials and methods

2.1. Materials and chemical

All chemicals and reagents used were of analytical grade obtained from Sigma-Aldrich for colloidal silica (Ludox HS40) and sodium hydroxide (NaOH), Ridel-de Haën for lead nitrate ($Pb(NO_3)_2$), Biochem Chemopharma for ethyl alcohol (C_2H_5OH) and Merck, Germany, for nitric acid (HNO_3). Stock solutions of lead(II) were prepared using lead nitrate in deionized water. The N-(2-methoxyphenyl)-N′-(2-methylphenyl)-thiourea (TMMe) and the N-(2-methoxyphenyl)-N′-(2-methoxyphenyl)-thiourea (TMM) were prepared in our laboratory as described a previous work [34]. The structural formulas of TMM and TMMe are given in Fig. 1. The solid adsorbent materials were prepared as described in Sections 2.1.1 and 2.1.2 of the present paper.

2.1.1. Preparation of Na-magadiite

The Na-magadiite is hydrothermally synthesized according to the literature [35]. A mixture of colloidal silica (Ludox 40), sodium hydroxide, deionized water, and ethyl alcohol, with a molar ratio of SiO_2:NaOH:

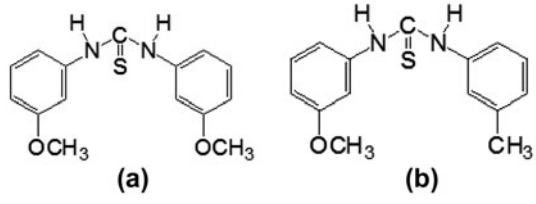

Fig. 1. Structural formulas of (a) TMM and (b) TMMe.

H_2O:C_2H_5OH = 1:0.13:14.17:1.78 was sealed in a Teflon-lined autoclave at 150˚C for 72 h. The product is filtered, washed carefully with distilled water, and dried at 80˚C for 24 h. The resulting white powder, named Mag, is characterized by XRD, infrared spectroscopy (FTIR), and SEM. Its cation exchange capacity (CEC) is measured according to the Kahr and Madsen method [36].

2.1.2. Preparation of thiourea derivatives intercalated Na-magadiite

The N-(2-methoxyphenyl)-N´-(2-methylphenyl)-thiourea (TMMe) and the N-(2-methoxyphenyl)-N´-(2-methoxyphenyl)-thiourea (TMM) were intercalated into the magadiite solid support according to the method developed recently as follows: 1 mmole of N-(2-methoxyphenyl)-N´-(2-methylphenyl)-thiourea (TMMe) [34] is added to a solution constituted from 20 ml of ethyl alcohol and 20 ml of distilled water. The mixture obtained is stirred for one hour at a temperature of 25˚C. One gram of as-synthesized Na-magadiite (Mag) was added to the precedent mixture and stirred up for one hour. The solid phase was separated by centrifugation and dried at 80˚C for 24 h. The resulting intercalated solid sample is called Mag/TMMe. The same procedure is used to obtain Mag/TMM in which TMM is N-(2-methoxyphenyl)-N´-(2-methoxyphenyl)-thiourea [34]. The obtained products (Mag/TMMe and Mag/TMM) are characterized by XRD, FTIR, and SEM.

2.2. Characterization methods

The XRD analysis is used to identify the materials obtained and to detect eventual changes which can occur on the solid samples after intercalation. The X-ray powder patterns were recorded using a Philips PW 1830 diffractometer with monochromatic Cu $K\alpha_1$ radiation (0.154 nm) in the region ranging from 2˚(2θ) to 40˚(2θ). The incorporation or not of the thiourea derivative compounds in the interlayer space of Na-magadiite is confirmed by infrared FTIR spectroscopy. A NICOLET 380 FTIR spectrometer is used. The solid samples are ground well to make KBr pellets under a hydraulic pressure of 600 kg/cm^2, and spectra are recorded in the range of 500–4000 cm^{-1}. In each scan, the amount of the solid sample and the amount of the KBr are kept constant in order to estimate the changes in the intensities of characteristics peaks with respect to the amount of thiourea loading. The scanning electron micrographs were obtained from a LEO-440A scanning electron microscope.

Thermo-gravimetric analyses (TGA, DTA) is carried out using a TA Instrument SDT 2960 thermoanalyzer between room temperature and 800˚C, at a heating rate of 5˚C/min. Reconstituted air (80% N_2 and 20% O_2) with a flow rate of 1 L/h is used during measurement. The chemical composition of the samples is performed by X-ray fluorescence using a Philips PW2540 Magix spectrophotometer yielding the percentage in weight of each constituting element.

For the analysis of aqueous solutions, a pH meter Hanna 210 microprocessor is used for pH measurements. Atomic absorption is used to determine the amount of residual metal in solution. It is one of the analytical methods which are currently used for analysis of metallic elements as traces. Experiments are carried out on a AA-660 Shimadzu corporation absorption spectrophotometer with an air/acetylene flame.

2.3. Equilibrium batch experiments

Equilibrium batch adsorption studies are carried out by exposing a suitable amount of the solid adsorbents to 100 ml solutions containing Pb(II) ions in sealed 150-ml Erlenmeyer flasks. The mixtures obtained are magnetically stirred at room temperature (25˚C). After equilibrium estimated for 1 h, the flasks are centrifuged and the supernatant are filtered through 0.45-μm membrane filters and analyzed by atomic absorption spectrophotometry. For kinetic studies, mixtures obtained by contacting 50 mg of adsorbent with 50 ml of 100 mg/l lead(II) solutions are stirred during 0–180 min. In order to establish the adsorption isotherms, 50 mg of adsorbent is contacted with lead(II) ions solutions at different concentrations. The latest concentrations ranged from 2 to 80 mg/l. However, the preliminary experiments show that the optimum mass of solid adsorbents in which the sorption capacity is maximum is equal to 50 mg. Furthermore, it is observed that the optimum pH value is function of the nature of the solid adsorbent used. For this purposes, lead(II) uptake experiments are conducted under two known and constant values of pH equals to 5 and 7. In these cases, pH of the solution is adjusted to the desired value by adding nitric acid (HNO_3) or sodium hydroxide as required. In all cases, amounts of lead(II) taken up by the adsorbent in each flask are determined by the following mass balance equation:

$$q = \frac{C_0 - C_f}{m} V \quad (1)$$

where q is the amount of lead(II) uptaken by the adsorbent (mg/g), C_0 is the initial lead(II) concentration in contact with the adsorbent (mg/dm^3), C_f is the lead(II) concentration (mg/dm^3) after the batch adsorption procedure, V is the volume of lead(II) solution (dm^3) in contact with the adsorbent, and m is the mass (g) of adsorbent.

3. Results and discussion

3.1. Characterization

3.1.1. X-ray diffraction

The XRD powder diffraction patterns of Mag, Mag/TMMe, and Mag/TMM solid samples are shown in Fig. 2. Fig. 2(a) gives the XRD powder diffraction pattern of the as-synthesized Na-magadiite used as the host matrix in the intercalation reactions. The recorded XRD pattern of Na-magadiite is typical of magadiite varieties, where all peak positions and relative intensities match perfectly the reported data [35,37], indicating that the product is highly crystalline and free from impurities. The basal spacing d_{001} of Mag is 1.56 nm. Following the intercalation of thiourea derivatives TMM and TMMe into Na-magadiite, it has been observed that, in addition to the characteristic peaks of the Na-magadiite, other peaks appear in the XRD powder diffraction patterns of Mag/TMMe and Mag/TMM solid samples, displayed, respectively, in Fig. 2(b) and (c). These additional peaks are assigned to TMM and TMMe species, confirming their intercalation into the solid support magadiite. Moreover, the presence of the peaks of the starting Na-magadiite material shows that the structure of this material is preserved after intercalation. This indicates that the intercalation of thiourea derivatives into the host matrix Na-magadiite does not change the original structure of magadiite. The same result was observed in the intercalation of magadiite by $[Pt(NH_3)_4]^{2+}$ [37] and $Co(sep)^{3+}$ ions [38].

3.1.2. Infrared FTIR spectroscopy

Fig. 3 shows the FTIR spectra of Mag, Mag/TMMe, and Mag/TMM. The FTIR spectrum of Na-magadiite displayed in Fig. 3(a) shows the presence of all

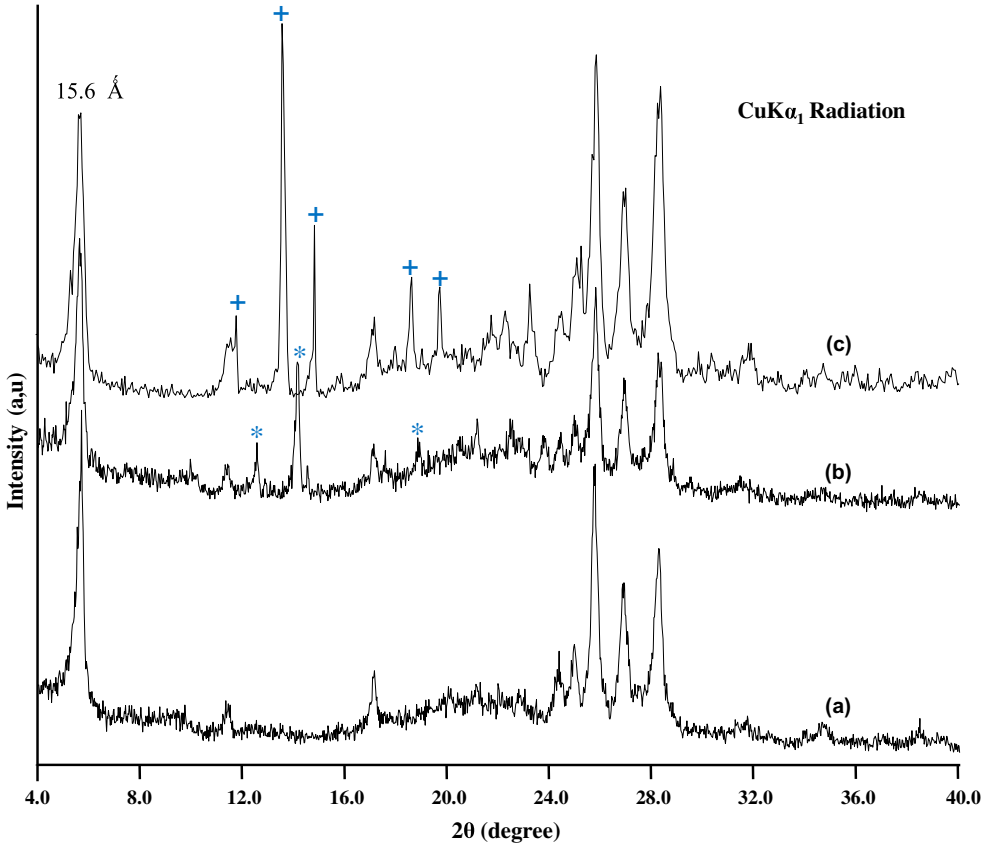

Fig. 2. Powder XRD patterns of (a) Mag, (b) Mag/TMMe, and (c) Mag/TMM (*: characteristic peaks of TMMe; +: characteristic peaks of TMM).

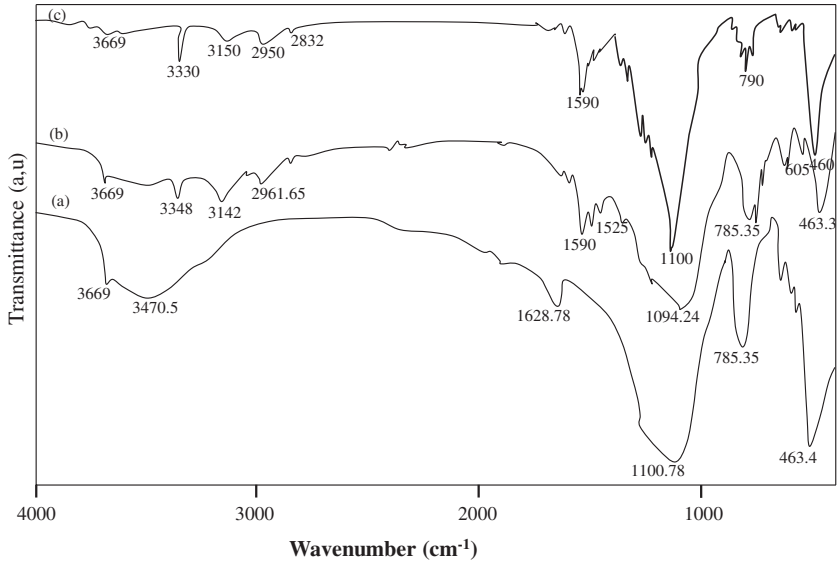

Fig. 3. Infrared (FTIR) spectra of (a) Mag, (b) Mag/TMMe, and (c) Mag/TMM.

vibrational bands characteristic of this material. Indeed, the small and sharp band appearing at 3,666 cm^{-1} is due to the weakly hydrogen-bonded free SiOH stretching of the isolated silanol groups present on the surface of Na-magadiite. These weakly bonded free SiOH groups is responsible for silylation reactions [22]. The broad vibrational band centered at 3,470 cm^{-1} is assigned to the OH stretching vibrations of interlamellar adsorbed water as well as to the strong hydrogen bonding SiOH stretching. Another characteristic bands are observed at 1,630 $cm^{-1}$and 785 cm^{-1} and may be assigned to the presence of physisorbed water and to the symmetric stretching vibrational mode of Si–O groups, respectively. The FTIR spectra of Mag/TMMe and Mag/TMM materials are displayed in Fig. 3(b) and (c), respectively. From these figures, one can observe the characteristic adsorption bands of Na-magadiite, the presence of others absorption bands at 3,348, 3,142, 2,961, and 1,525 cm^{-1}. These absorption bands are assigned to the stretching vibrational mode of the N–H groups, the C–H stretching vibration of the aromatic groups, the C–H stretching vibration of the methyl groups and the C=C stretching vibration, respectively, and are due to the presence of thiourea compounds into the solid samples. These results confirm the presence of thiourea derivatives, TMM and TMMe, in interlayer space of magadiite and shows that the intercalated solid samples, Mag/TMM and Mag/TMMe, retain the structure of the Na-magadiite material. However, it is important to note that the infrared spectra of TMM and TMMe (not shown here) are very similar, which does not allow to differentiate between them by infrared analysis. Therefore, it is also difficult to differentiate between Mag/TMM and Mag/TMMe by this analysis method.

3.1.3. Chemical and thermal analysis

The chemical compositions of Mag, Mag/TMM, and Mag/TMMe solid samples are determined by combining chemical and thermal analysis. The results are given in Table 1. The chemical formula of the as-synthesized Na-magadiite (Mag sample) is a characteristic of such a material and agrees well with the idealized one reported in the literature [17]. Determining the chemical formulas Mag/TMM and Mag/TMMe confirms the presence of TMM and TMMe, respectively, in both materials and shows that both materials retain the structure of the starting Na-magadiite after intercalation. The calculated chemical formulas show also that the amount of TMM inserted in Na-magadiite is greater than that of TMMe. This could certainly have an influence on lead adsorption reaction.

3.1.4. Scanning electron microscopy

Fig. 4 shows the morphology of Mag, Mag/TMMe, and Mag/TMM. The Mag sample is formed of silicate layers intergrown to form spherical nodules resembling rosettes, which consist of aggregated thin platelets (Fig. 4(a)). No impurity is detected. After intercalation with TMMe and TMM, Fig. 4(b)

Table 1
Chemical composition of Mag, Mag/TMMe, and Mag/TMM solid samples

Sample	Na_2O[a] (wt%)	SiO_2[a] (wt%)	Organic content[a] (wt%)	H_2O[b] (wt%)	Chemical formula[c]
Mag	6.394	80.295	–	13.31	$Na_2Si_{14}O_{29}$·7.73 H_2O
Mag/TMMe	5.238	70.962	13.65	10.15	$Na_2Si_{14}O_{29}$·0.594 TMMe·6.68 H_2O
Mag/TMM	5.276	65.614	21.78	07.33	$Na_2Si_{14}O_{29}$·0.968 TMMe·5.21 H_2O

[a]Determined from chemical analysis.
[b]Determined from thermal analysis.
[c]Determined by combining chemical and thermal analyses.

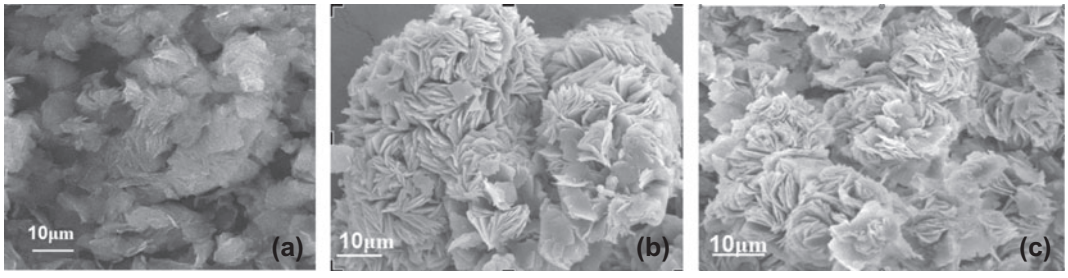

Fig. 4. SEM of (a) Mag, (b) Mag/TMMe, and (c) Mag/TMM.

and (c), respectively, the morphology of the starting Na-magadiite material is maintained. However, the rosettes become more open and the platelets are thicker than those observed for Na-magadiite. This result confirms the presence of thiourea organic compounds into solid probably intercalated in the interlayer space.

3.1.5. The cation exchange capacity determination

CEC is measured in order to evaluate the potential use of the as-synthesized Na-magadiite material for intercalation and also for organofunctionalization process. The CEC determination was carried out using the conductometric method developed by Kahr and Madsen [36]. After calculation, an experimental CEC value of 116.5 meq/100 g of Na-magadiite is obtained. This value is in good agreement with that reported in the literature [19] and indicates that the as-synthesized magadiite material obtained is of high quality as observed by XRD, FTIR and SEM analysis.

3.2. Kinetic studies

The study of adsorption kinetics is an important feature to be considered in aqueous effluent treatments as it provides valuable information about the mechanism of adsorption processes. In the present work, two kinetic models are applied in order to understand and then explain the experimentally obtained data. They are namely the first-order and pseudo-second-order models. The linear form of the first-order equation of the Lagergren model [39] is given by the following equation:

$$\log(q_e - q_t) = \log(q_e) - \frac{k_1 \cdot t}{2,303} \quad (2)$$

where k_1 is the rate constant of adsorption (min^{-1}), and q_e and q_t are the adsorption loading of lead(II) (mg/g) at equilibrium and at time t (min), respectively. The equilibrium loading q_e (mg/g) is calculated from the langmuir adsorption isotherm. By plotting, $\log(q_e - q_t)$ against t, a straight line is obtained and the value of the rate constant k_1 can be calculated.

The pseudo-second-order equation (Ho and Mc Kay) [40] is expressed as:

$$\frac{t}{q_t} = \frac{1}{k_2 q_e^2} + \frac{1}{q_e} t \quad (3)$$

where k_2 (g/mg min) is the rate constant of pseudo-second-order adsorption. Plotting t/q_t against t, a linear function is obtained and the rate constant k_2 as well as q_e can be calculated.

The behavior of lead(II) adsorption kinetics on Mag, Mag/TMMe, and Mag/TMM materials are

shown in Fig. 5. The adsorption of lead(II) increases relatively quickly up to 30 min and slowly increases as equilibrium was reached. The lead(II) uptake becomes almost constant after 60 min for all the materials used. This can be explained by the existence of the exposed reactive basic centers for interaction on the readily accessible surfaces. However, as the coverage increases, the number of available surface sites for the adsorption decreases until it reaches equilibrium.

The simulated plots for the first-order and pseudo-second-order models are shown in Fig. 6(a) and (b), respectively. The kinetic data for adsorption of lead(II) onto Mag, Mag/TMMe and Mag/TMM obtained from the related plots are collected in Table 2.

It is clearly shown that pseudo-second-order kinetic plot presents a better regression coefficients ($R^2 > 0.999$) at pH 7 and pH 5 for all adsorbents samples, which suggests that the adsorption kinetic can be described by the pseudo-second-order rate equation perfectly. This result implies that chemisorption is predominant and may be considered as the limiting rate-step which control the adsorption process.

3.3. Adsorption isotherms

The capacity of these materials to remove lead(II) from water is evaluated by adsorption isotherms process. The lead(II) adsorption isotherms at pH 5 and pH 7 are given in Fig. 7. The latter shows that the amount of lead(II) uptake increases with increasing equilibrium concentration until a plateau is reached for all adsorbents samples. The maximum of adsorption is observed for the Mag/TMM sample at pH 5. In order to understand and then explain the adsorption phenomenon, the Langmuir [41] and Freundlich [42] theoretical models are applied to fit the experimental data.

The Langmuir model assumes a monolayer adsorption of molecules of adsorbate onto an ideal solid surface composed by distinct adsorption sites with uniform adsorption energies. The adsorbates are immobile on the surface, and there are no interactions between adsorbates molecules on adjacent sites. The linear form of the Langmuir model is represented by the following equation:

$$\frac{1}{x/m} = \frac{1}{Q_0 b}\frac{1}{C_e} + \frac{1}{Q_0} \tag{4}$$

where x/m (mg/g) is the quantity of metal ions (mg) adsorbed, per gram of solid, from the aqueous solution; C_e (mg/l) is the equilibrium concentration of metal ions in aqueous solution; b is the Langmuir equilibrium constant and Q_0 (mg/g) is the maximum adsorption capacity. The two last parameters are determined from the linearized Langmuir plots displayed in Fig. 8.

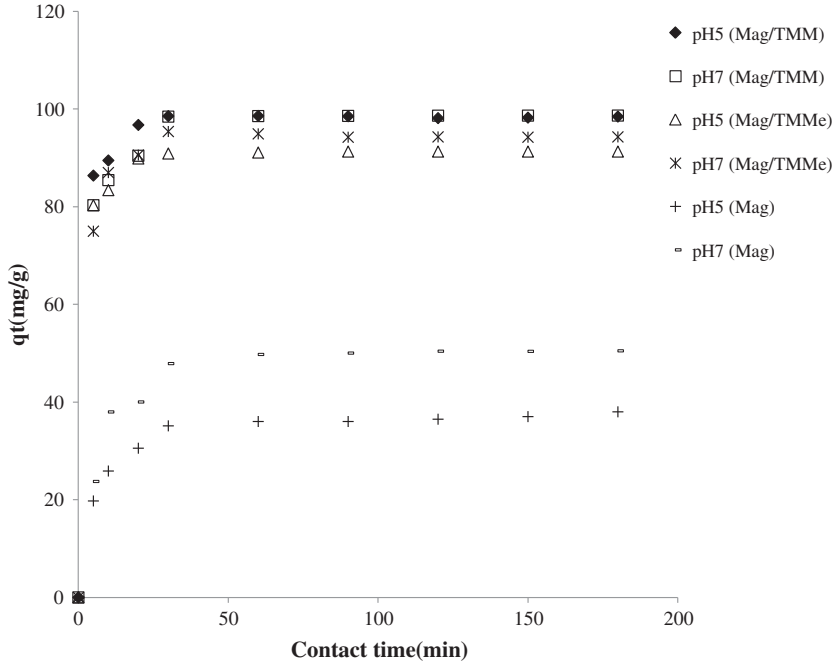

Fig. 5. Effect of contact time for lead(II) adsorption onto Mag, Mag/TMMe, and Mag/TMM at pH 5 and pH 7.

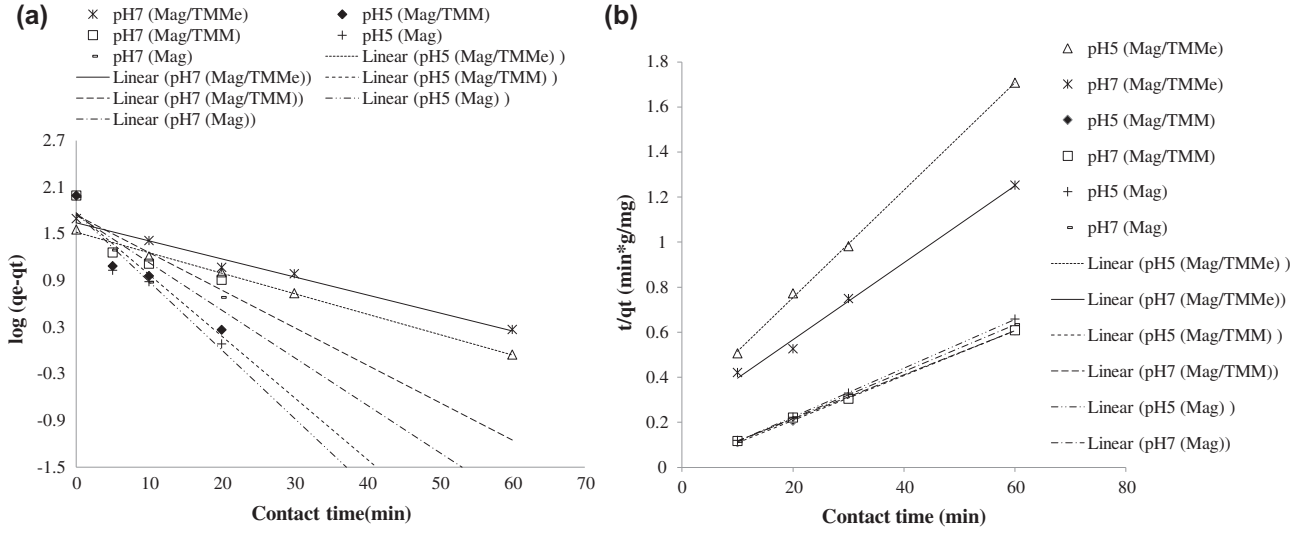

Fig. 6. Kinetics of lead(II) removal onto Mag, Mag/TMMe, and Mag/TMM at pH 5 and pH 7, according to (a) first-order model and (b) pseudo-second-order model.

Table 2
Kinetic parameters for the adsorption of lead(II) ions onto Mag, Mag/TMMe, and Mag/TMM at pH 5 and pH 7

		First-order kinetic model		Pseudo-second-order kinetic model	
Adsorbent	pH	R_1^2	k_1 (min^{-1})	R_2^2	k_2 (g mg^{-1} min^{-1})
Mag	5	0.9218	0.0381	0.9999	0.014
	7	0.8305	0.0264	0.9999	0.0083
Mag/TMMe	5	0.9975	0.060	0.999	0.0020
	7	0.9855	0.053	0.994	0.0013
Mag/TMM	5	0.9076	0.0343	0.9999	0.0117
	7	0.8691	0.0367	0.9993	0.006

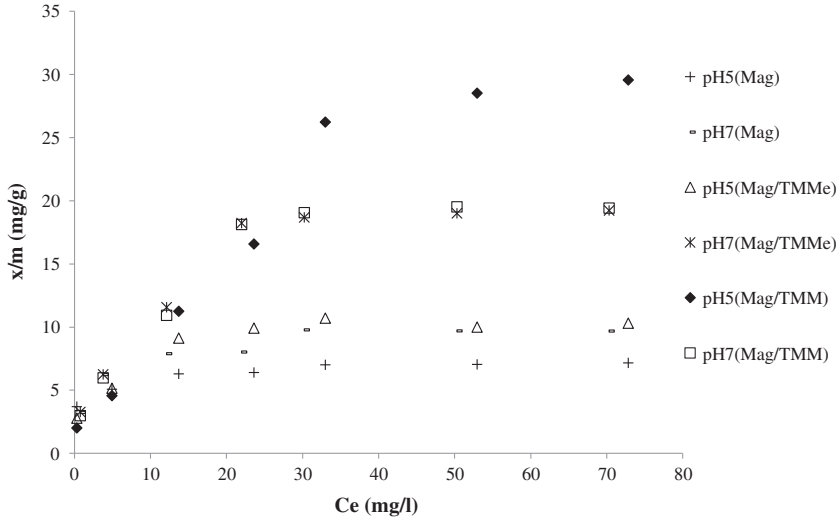

Fig. 7. Isotherms of lead(II) adsorption onto Mag, Mag/TMMe, and Mag/TMM at pH 5 and pH 7.

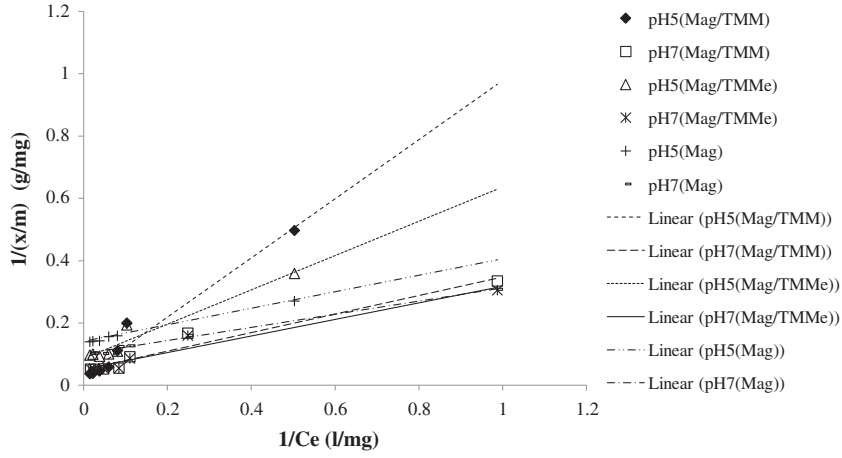

Fig. 8. Langmuir plots for lead(II) adsorption onto Mag, Mag/TMMe, and Mag/TMM at pH 5 and pH 7.

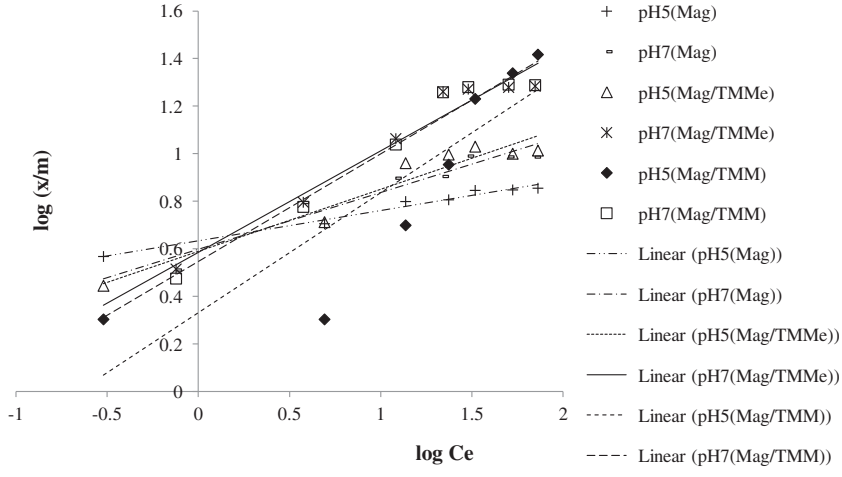

Fig. 9. Freundlich plots for lead(II) adsorption onto Mag, Mag/TMMe, and Mag/TMM at pH 5 and pH 7.

Table 3
Langmuir and Freundlich parameters for lead(II) ions removal onto Mag, Mag/TMMe, and Mag/TMM

		Freundlich constants			Langmuir constants			
Adsorbent	pH	k	n	R^2	Q_0 (mg/g)	b (L/g)	R^2	R_L
Mag	5	1.43	7.88	0.98	7.358	0.49963	0.9837	0.0244
	7	1.77	4.18	0.9251	9.910	0.47616	0.9946	0.0256
Mag/TMMe	5	1.94	3.83	0.9361	13.28	0.13432	0.9735	0.0851
	7	1.54	2.34	0.9556	19.92	0.19339	0.9552	0.0607
Mag/TMM	5	1.13	1.98	0.7715	33.44	0.03152	0.9600	0.2839
	7	1.75	2.21	0.9583	19.417	0.26868	0.9611	0.0267

Table 4
Comparison of the maximum adsorption capacity of Pb(II) ions on some natural and synthetic adsorbents from aqueous solution

Adsorbent	Q_0 (mg/g)	Ref.
Organophilic bentonite	22	[43]
Natural smectite "CL"	1,061.91 ± 0.15	[44]
AL/Z_R-PILC$_{APT-723}$	2,676.51 ± 0.11	[44]
AL/Z_R-PILC$_{APT-823}$	2,477.79 ± 0.13	[44]
Cancrinite-type zeolite	523.71	[45]
Chitosan	7.452	[46]
Hazelnut husks activated carbon (ACHH)	13.05	[47]
Pine cone activated carbon	27.53	[48]
Spirogyra neglecta	55.70	[49]
Ethylenediamine-modified attapulgite (EMATP)	258	[50]
TMA-birnessite	263.18	[51]
Ca–Al layered double hydroxides (LDHs)	972.9	[52]
Calcium phosphates (CaP)	1,226	[53]
Kaolinite	11.52	[54]
Poly(hydroxyl)zirconium modified kaolinite	9.01	[54]
Montmorillonite	31.05	[54]
Poly(hydroxyl)zirconium modified montmorillonite	31.44	[54]
Natural bentonite	0.015	[55]
Clay/poly(methoxyethyl)acrylamide (PMEA)	81.02	[56]
Mag	9.91	This work
Mag/TMMe	19.41	This work
Mag/TMM	33.44	This work

The Freundlich isotherm is merely empirical and at best describes the adsorption on heterogeneous surfaces. The linear form of the Freundlich model is expressed by the following equation:

$$\log \frac{x}{m} = \frac{1}{n} \log C_e + \log k \quad (5)$$

where x/m (mg/g) is the quantity of metal ions (mg) adsorbed, per gram of solid, from the aqueous solutions. C_e (mg/l) is the equilibrium concentration of metal ions in aqueous solution. n and k are the Freundlich constants. Both are calculated from the simulated plots shown in Fig. 9.

The isotherm constants for lead(II) adsorption onto the three adsorbent at pH 5 and pH 7 are summarized in Table 3. It appears that the determination coefficients obtained at pH 5 and 7 by the Langmuir model are better than those observed for the Freundlich model at the same pH values, indicating a good fit to the Langmuir model than the Freundlich model. In the case of Langmuir model, the determination of the separation parameter, R_L, can give additional information on the adsorption reaction that allow to explain the experimental data. This parameter is defined as:

$$R_L = \frac{1}{(1 + bC_0)}$$

where b is the Langmuir constant, and C_0 is the highest initial concentration of metal in aqueous solutions. It is indicative of the isotherm shape and predicts the feature of the adsorption. It can take several values. Indeed, in function of the value of R_L, the adsorption is considered as irreversible ($R_L = 0$), favorable ($0 < R_L < 1$), linear ($R_L = 1$), or unfavorable ($R > 1$). As shown in Table 3, the calculation of the separation factor, R_L, gives values between 0.0244 and 0.2839 which confirm that the three adsorbents show favorable adsorption for lead(II) ions.

The two intercalated materials (Mag/TMM and Mag/TMMe) exhibit higher adsorption capacities than the starting material (Mag). The maximum adsorption capacity of lead(II) determined by the Langmuir model equals 33.9 mg/g (0.1615 mmol g^{-1}) and is observed at pH 5 for Mag/TMM material. At pH 7, this value equals 19.9 mg g^{-1} for the Mag/TMMe material. As shown in Table 4, the results obtained compare well with the literature and the adsorbents materials used in the present work may constitute a

good alternative for lead(II) adsorption, especially for low concentration of the metal in aqueous solutions.

4. Conclusion

In this work, Na-magadiite was synthesized and then modified by organic Thiourea derivatives molecules (TMMe and TMM). The products were characterized by different analysis methods and used for the removal of lead(II) from aqueous solutions. It was found that the variation of pH affects the adsorption capacity of the metal. The kinetics of adsorption of metal ions were experimentally studied, and the obtained rate data were analyzed using simple kinetic models. The results clearly demonstrate that the pseudo-second-order adsorption mechanism is predominant, which led us to conclude that the adsorption process is controlled by a chemical adsorption process. Equilibrium isotherms have been determined using Langmuir and Freundlich mathematics equations. The study shows that the results fit well the Langmuir model. Compared to the starting Na-magadiite, all the studied materials display high adsorption capacities. The most important value equals 33.44 mg/g and is observed for Mag/TMM at pH 5.

List of symbols

q	—	amount of lead(II) uptake by the adsorbent (mg/g)
C_0	—	initial lead(II) concentration in contact with the adsorbent (mg/dm^3)
C_f	—	lead(II) concentration (mg/dm^3) after the batch adsorption procedure
V	—	volume of lead(II) solution (dm^3) in contact with the adsorbent
M	—	mass (g) of adsorbent
q_e	—	adsorption loading of lead(II) (mg/g) at equilibrium
q_t	—	adsorption loading of lead(II) (mg/g) at time t (min)
k_1	—	rate constant of adsorption (min^{-1})
k_2	—	rate constant of pseudo-second-order adsorption (g/mg min)
x/m	—	quantity of metal ions (mg) adsorbed, per gram of solid (mg/g)
Q_0	—	the maximum adsorption capacity
b	—	the Langmuir equilibrium constant
C_e	—	the equilibrium concentration of metal ions in aqueous solution (mg/l)
k	—	the Freundlich constant

References

[1] J.R. Parga, G. González, H. Moreno, J.L. Valenzuela, Thermodynamic studies of the strontium adsorption on iron species generated by electrocoagulation, Desalin. Water Treat. 37 (2013) 244–252.

[2] C.M. Futalan, C.C. Kan, M.L. Dalida, K.J. Hsien, C. Pascua, M.W. Wan, Comparative and competitive adsorption of copper, lead and nickel using chitosan immobilized on bentonite, Carbohydr. Polym. 83 (2011) 528–536.

[3] F. Fu, Q. Wang, Removal of heavy metal ions from wastewaters: A review, J. Environ. Manage. 92 (2011) 407–418.

[4] L. Lebrun, F. Vallée, B. Alexandre, Q.T. Nguyen, Preparation of chelating membranes to remove metal cations from aqueous solutions, Desalination 207 (2007) 9–23.

[5] M.J. Jung, P. Venkateswaran, Y.S. Lee, Solvent extraction of nickel(II) ions from aqueous solutions using triethylamine as extractant, J. Ind. Eng. Chem. 14 (2008) 110–115.

[6] T.G. Chuah, A. Jumasiah, I. Azni, S. Katayon, S.Y. Thomas Choong, Rice husk as a potentially low-cost biosorbent for heavy metal and dye removal: An overview, Desalination 175 (2005) 305–316.

[7] D. Kavak, Removal of lead from aqueous solutions by precipitation: Statistical analysis and modeling, Desalin. Water Treat. 51 (2013) 1720–1726.

[8] C. Ye, H. Yang, J. Lin, H. Zeng, F. Yu, Study on ion exchange property of removing Mn^{2+} and Fe^{2+} in groundwater by modified zeolite, Desalin. Water Treat. 30 (2011) 114–121.

[9] Ö. Arar, Removal of lead(II) from water by di (2-ethylhexyl) phosphate containing ion exchange resin, Desalin. Water Treat. 52 (2014) 3197–3205.

[10] D. Kavak, M. Demir, B. Başsayel, A.S. Anagün, Factorial experimental design for optimizing the removal of lead ions from aqueous solutions by cation exchange resin, Desalin. Water Treat. 51 (2013) 1712–1719.

[11] N.G. Kandile, A.S. Nasr, Environment friendly modified chitosan hydrogels as a matrix for adsorption of metal ions, synthesis and characterization, Carbohydr. Polym. 78 (2009) 753–759.

[12] M.L.P. Dalida, A.F.V. Mariano, C.M. Futalan, C.C. Kan, W.C. Tsai, M.W. Wan, Adsorptive removal of Cu (II) from aqueous solutions using non-crosslinked and crosslinked chitosan-coated bentonite beads, Desalination 275 (2011) 154–159.

[13] P. Xu, G.M. Zeng, D.L. Huang, C.L. Feng, S. Hu, M.H. Zhao, C. Lai, Z. Wei, C. Huang, G.X. Xie, Z.F. Liu, Use of iron oxide nanomaterials in wastewater treatment: A review, Sci. Total Environ. 424 (2012) 1–10.

[14] A. Kamari, W.S. Wan Ngah, Isotherm, kinetic, and thermodynamic studies of lead and copper uptake by H_2SO_4 modified chitosan, Colloids Surf. B: Biointerfaces 73 (2009) 257–266.

[15] P. Heinrich Thiesen, K. Beneke, G. Lagaly, Silylation of a crystalline silicic acid: An MAS NMR and porosity study, J. Mater. Chem. 12 (2002) 3010–3015.

[16] F. Feng, K.J. Balkus Jr., Direct synthesis of ZSM-5 and mordenite using poly(ethylene glycol) as a structure-directing agent, J. Porous Mater. 10 (2003) 235–242.

[17] S. Okutomo, K. Kuroda, M. Ogawa, Preparation and characterization of silylated magadiites, Appl. Clay Sci. 15 (1999) 253–264.
[18] S.F. Wang, M.L. Lin, Y.N. Shieh, Y.R. Wang, S.J. Wang, Organic modification of synthesized clay-magadiite, Ceram. Int. 33 (2007) 681–685.
[19] K. Beneke, G. Lagaly, Kenyaite-synthesis and properties, Am. Min. 68 (1983) 818–826.
[20] F. Kooli, L. Mianhui, S.F. Alshahateet, F. Chen, Z. Yinghuai, Characterization and thermal stability properties of intercalated Na-magadiite with cetyltrimethylammonium (C_{16}TMA) surfactants, J. Phys. Chem. Solids 67 (2006) 926–931.
[21] I. Fujita, K. Kuroda, M. Ogawa, Synthesis of interlamellar silylated derivatives of magadiite and the adsorption behavior for aliphatic alcohols, Chem. Mater. 15 (2003) 3134–3141.
[22] K.W. Park, J.H. Jung, S.K. Kim, O.Y. Kwon, Interlamellar silylation of magadiite by octyl triethoxysilane in the presence of dodecylamine, Appl. Clay Sci. 46 (2009) 251–254.
[23] D.L. Guerra, A.A. Pinto, J.A. de Souza, C. Airoldi, R.R. Viana, Kinetic and thermodynamic uranyl(II) adsorption process into modified Na-magadiite and Na-kanemite, J. Hazard. Mater. 166 (2009) 1550–1555.
[24] D.L. Guerra, A.A. Pinto, R.R. Viana, C. Airoldi, Modification of magadiite surface by organofunctionalization for application in removing As(V) from aqueous media: Kinetic and thermodynamic, Appl. Clay Sci. 256 (2009) 702–709.
[25] Á. Fudala, Z. Kónya, Y. Kiyozumi, S.-I. Niwa, M. Toba, F. Mizukami, P.B. Lentz, J. Nagy, I. Kiricsi, Preparation, characterization and application of the magadiite based mesoporous composite material of catalytic interest, Microporous Mesoporous Mater. 35–36 (2000) 631–641.
[26] G. Pál-Borbély, H.K. Beyer, Y. Kiyozumi, F. Mizukami, Recrystallization of magadiite varieties isomorphically substituted with aluminum to MFI and MEL zeolites, Microporous Mater. 11 (1997) 45–51.
[27] O.Y. Kwon, H.S. Shin, S.W. Choi, Preparation of porous silica-pillared layered phase: Simultaneous intercalation of amine-tetraethylorthosilicate into the H^+-magadiite and intragallery amine-catalyzed hydrolysis of tetraethylorthosilicate, Chem. Mater. 12 (2000) 1273–1278.
[28] S. Peng, Q. Gao, Z. Du, J. Shi, Precursors of TAA-magadiite nanocomposites, Appl. Clay Sci. 31 (2006) 229–237.
[29] D.L. Guerra, A.A. Pinto, C. Airoldi, R.R. Viana, Adsorption of uranyl(II) into modified lamellar Na-kanemite, Inorg. Chem. Commun. 11 (2008) 539–544.
[30] D.L. Guerra, C. Airoldi, R.R. Viana, Retracted: Modification of hectorite by organofunctionalization for use in removing U(VI) from aqueous media: Thermodynamic approach, J. Environ. Radioact. 101 (2010) 122–133.
[31] B. Royer, N.F. Cardoso, E.C. Lima, T.R. Macedo, C. Airoldi, Sodic and acidic crystalline lamellar magadiite adsorbents for the removal of methylene blue from aqueous solutions: Kinetic and equilibrium studies, Sep. Sci. Technol. 45 (2009) 129–141.
[32] N. Miyamoto, R. Kawai, K. Kuroda, M. Ogawa, Intercalation of a cationic cyanine dye into the layer silicate magadiite, Appl. Clay Sci. 19 (2001) 39–46.
[33] M. Ogawa, Photoisomerization of azobenzene in the interlayer space of magadiite basis of a presentation given at materials discussion No. 5, 2225 September 2002, Madrid, Spain, J. Mater. Chem. 12 (2002) 3304–3307.
[34] M. Bouchekara, A. Djafri, N. Vanthuyne, C. Roussel, Atropisomerism in some N,N´-diaryl-2-iminothiazoline derivatives: Chiral separation and configurational stability, Arkivoc 2002 (2002) 72–79.
[35] M. Sassi, J. Miehé-Brendlé, J. Patarin, A. Bengueddach, Na-magadiite prepared in a water/alcohol medium: Synthesis, characterization and use as a host material to prepare alkyltrimethylammonium- and Si-pillared derivates, Clay Min. 40 (2005) 369–378.
[36] G. Kahr, F.T. Madsen, Determination of the cation exchange capacity and the surface area of bentonite, illite and kaolinite by methylene blue adsorption, Appl. Clay Sci. 9 (1995) 327–336.
[37] W. Schwieger, T. Selvam, O. Gravenhorst, N. Pfänder, R. Schlögl, G.T.P. Mabande, Intercalation of $[Pt(NH_3)_4]^{2+}$ ions into layered sodium silicate magadiite: A useful method to enhance their stabilisation in a highly dispersed state, J. Phys. Chem. Solids 65 (2004) 413–420.
[38] J.S. Dailey, T.J. Pinnavaia, Intercalative reaction of a cobalt(III) cage complex, $Co(sep)^{3+}$, with magadiite, a layered sodium silicate, J. Inclusion Phenom. Mol. Recognit. Chem. 13 (1992) 47–61.
[39] S. Lagergren, About the theory of so-called adsorption of soluble substances, K. Sven Vetenskapsakad Handl. 24 (1898) 1–39.
[40] Y.S. Ho, D.A.J. Wase, C.F. Forster, Kinetic studies of competitive heavy metal adsorption by sphagnum moss peat, Environ. Technol. 17 (1996) 71–77.
[41] I. Langmuir, The constitution and fundamental properties of solids and liquids. Part I. solids, J. Am. Chem. Soc. 38 (1916) 2221–2295.
[42] H.M.F. Freundlich, Über die adsorption in lösungen, Z. Phys. Chem. 57 (1906) 385–470.
[43] S. Andini, R. Cioffi, F. Montagnaro, F. Pisciotta, L. Santoro, Simultaneous adsorption of chlorophenol and heavy metal ions on organophilic bentonite, Appl. Clay Sci. 31 (2006) 126–133.
[44] D.L. Guerra, C. Airoldi, Kinetics and modified clay thermodynamic from the Brazilian amazon region for lead removal, J. Hazard. Mater. 159 (2008) 412–419.
[45] W. Qiu, Y. Zheng, Removal of lead, copper, nickel, cobalt, and zinc from water by a cancrinite-type zeolite synthesized from fly ash, Chem. Eng. J. 145 (2009) 483–488.
[46] J.R. Rangel-Mendez, R. Monroy-Zepeda, E. Leyva-Ramos, P.E. Diaz-Flores, K. Shirai, Chitosan selectivity for removing cadmium(II), copper(II), and lead(II) from aqueous phase: pH and organic matter effect, J. Hazard. Mater. 162 (2009) 503–511.
[47] M. Imamoglu, O. Tekir, Removal of copper(II) and lead(II) ions from aqueous solutions by adsorption on activated carbon from a new precursor hazelnut husks, Desalination 228 (2008) 108–113.
[48] M. Momčilović, M. Purenović, A. Bojić, A. Zarubica, M. Ranđelović, Removal of lead(II) ions from aqueous solutions by adsorption onto pine cone activated carbon, Desalination 276 (2011) 53–59.

[49] A. Singh, D. Kumar, J.P. Gaur, Continuous metal removal from solution and industrial effluents using *Spirogyra* biomass-packed column reactor, Water Res. 46 (2012) 779–788.
[50] Y. Deng, Z. Gao, B. Liu, X. Hu, Z. Wei, C. Sun, Selective removal of lead from aqueous solutions by ethylenediamine modified attapulgite, Chem. Eng. J. 223 (2013) 91–98.
[51] C.-Y. Lee, T. Kim, S. Komarneni, S.-K. Han, Y. Cho, Sorption characteristics of lead cations on microporous organo-birnessite, Appl. Clay Sci. 83–84 (2013) 263–269.
[52] R. Rojas, Copper, lead and cadmium removal by Ca Al layered double hydroxides, Appl. Clay Sci. 87 (2014) 254–259.
[53] D. Pham Minh, N.D. Tran, A. Nzihou, P. Sharrock, Calcium phosphate based materials starting from calcium carbonate and orthophosphoric acid for the removal of lead(II) from an aqueous solution, Chem. Eng. J. 243 (2014) 280–288.
[54] S.S. Gupta, K.G. Bhattacharyya, Interaction of metal ions with clays: I. A case study with Pb(II), Appl. Clay Sci. 30 (2005) 199–208.
[55] R. Donat, A. Akdogan, E. Erdem, H. Cetisli, Thermodynamics of Pb^{2+} and Ni^{2+} adsorption onto natural bentonite from aqueous solutions, J. Colloid Interface Sci. 286 (2005) 43–52.
[56] M. Şölener, S. Tunali, A.S. Özcan, A. Özcan, T. Gedikbey, Adsorption characteristics of lead(II) ions onto the clay/poly(methoxyethyl)acrylamide (PMEA) composite from aqueous solutions, Desalination 223 (2008) 308–322.